



OPEN

Temperature based maximum power point tracking for photovoltaic modules

Josean Ramos-Hernanz, Irantzu Uriarte, Jose Manuel Lopez-Guede, Unai Fernandez-Gamiz, Amaia Mesanza & Ekaitz Zulueta

In this article authors propose a temperature based Maximum Power Point Tracking algorithm (MPPT). Authors show that there is an optimal current vs maximum power curve that depends on photovoltaic (PV) module temperature. Therefore, the maximum power point (MPP) can be achieved in very few commutation steps if the control forces the PV module to work in temperature dependent optimal curve. Authors shows how this PV module temperature based MPPT is stable and converges to MPP for each temperature. In order to proof its stability, authors propose a Lyapunov energy function. This Lyapunov energy function has positive values for all values except into MPP given the PV module temperature. This Lyapunov energy function has negative increment along each time step. Hence, the stability of temperature based MPPT can be demonstrated. The proposed MPPT algorithm proposes a current set point. This current set point is obtained with instantaneous PV module power and temperature dependent maximum power vs optimal current curve. Stability is analysed for different temperature levels. Optimal current vs maximum power curve has been modelled by a line. The lines' coefficients depend on PV module temperature. Proposed Lyapunov energy function is not symmetric about equilibrium or MPP because MPPT algorithm and PV module dynamic have no symmetric behaviour about this equilibrium point.

Photovoltaic market shows a steady and continuous growth worldwide. This advance is possible thanks to the large reduction of the cost and to the efficiency increase of commercial photovoltaic modules. A growth around 20% has been achieved in the recent years in the world photovoltaic market. A descending trend in the price of the modules and other basic components of the photovoltaic facilities has been observed since 2010. In this context, photovoltaic energy has become a feasible alternative to deal with the growing request of energy.

An efficient MPPT algorithm is a key issue to improve the energy incomes of photovoltaic panels in addition to increase overall system efficiency. Its fundamental advantage based on neural networks for modelling is that no prior knowledge of the physical parameters related to the PV system is required¹. Lopez-Guede et al.² presented a neural networks based model of a PV module Mitsubishi Electric PV-TD185MF5 (185 Wp) which is located on the roof of the Faculty of Engineering of Vitoria-Gasteiz (University of the Basque Country, Spain). A data set of 63,000 samples collected during 18 months (from August 2013 to February 2015) has been used. That is the model used in present work.

Nowadays, several methods are being used to get the maximum energy from the solar cells³. Dang et al.⁴ increased the efficiency of the nanowire CdS/CdTe solar cell from 9 to 11% by using a 10 nm thick molybdenum oxide as a transparent layer. On the other hand, single axis and dual axis solar trackers are also used to enhance the solar insolation collection capability by orienting the solar⁵. While various Maximum Power Point Tracking (MPPT) algorithms such as Incremental Conductance (IC) algorithm⁵⁻⁷, Perturb and Observe (P&O)⁸⁻¹⁰, Artificial Neural Network (ANN)¹⁰, fuzzy logic¹¹, and Particle Swarm Optimization (PSO)¹². A review of the MPPT based on PV panel and power converter characteristics can be found in Motahhir et al.¹³.

The P&O algorithm requires a reduced implementation cost with good performance. This algorithm can effectively address stable variations around the MPP and dynamic variations of the environmental conditions such as temperature and solar radiation¹⁴. Likewise, Alik et al.¹⁵ uses this algorithm because they also consider that the main advantages of this method are its low cost, simplicity and precision. To improve the performance of the installation, Moshksar et al.¹⁶ proposed a new MPPT algorithm comparing it with several versions of P&O.

University of the Basque Country, UPV/EHU, Vitoria-Gasteiz, Spain. email: ekaitz.zulueta@ehu.es

In the case of Ramos-Hernanz et al.¹⁷, they compare the behaviour of three versions of the algorithm P&O in simulation and in real life.

Other authors use the IC MPPT control algorithm, because it measures precisely the temperature of the PV module and tracks the MPP without oscillations⁵. In the opinion of Chen et al.¹⁸, the IC control algorithm improves the behaviour of the P&O. In the case of Radjai et al.¹⁹ they develop a new IC controller based on fuzzy logic with direct control to eliminate all the disadvantages of the classic control algorithm IC. In Ramos-Hernanz et al.²⁰ the behaviour of the IC algorithm in simulation and in a real installation is compared. In the work of Rezk et al.²¹ four of these MPPT are compared: P&O, IC, Hill Climbing (HC) and Fuzzy Logic Controller (FLC). In the case of Cortajarena et al.²² the algorithms used are HC, P&O and a new Sliding Mode Control (SMC) algorithm.

A new MPPT based technique that combines simplicity and effectiveness was proposed by Chaieb et al.²³. The proposed method combines the Simplified Accelerated Particle Swarm Optimization (SAPSO), which is a variant of the Particle Swarm Optimization (PSO) algorithm and the classic HC algorithm.

According to Li²⁴, the P&O and IC methods are the most used. The P&O method can work well when solar irradiance and temperature do not change rapidly over time. Low cost P&O based controller can be implemented with a simple analogue circuit or microcontroller. But this method has the disadvantage that it cannot track the MPP quickly and the output power oscillates around the MPP. The method IC has a better performance than the algorithm P&O but its implementation is more difficult. In Bayod-Rujula et al.²⁵, researchers ensure that control algorithms P&O and IC are the most used due to their simplicity. However, these algorithms have some weaknesses that affect their efficiency, especially when there are rapid changes in irradiance or partial shading of the installation. In order to solve some of the problems presented by the algorithm P&O, Li et al.²⁶ proposed an MPPT control strategy with Variable Climate Parameters (VWP), which has the ability to track the MPP more quickly and compares this new algorithm to the P&O algorithms and with the fuzzy control method. However, Jamal et al.²⁷ compared a new control algorithm based on Finite Time Sliding Mode Control (FTSMC) with the P&O methods and the standard SMC algorithm.

One of the main problems in PV installations is the control of the MPPT when there are partial shading conditions. Mohapatra et al.²⁸ perform a very thorough review of all modern MPPT algorithms that are used in PV installations, reaching the conclusion that the choice of MPPT control algorithm depends on the application, hardware availability, cost, convergence time, accuracy and reliability of the system. In the study of Hadji et al.²⁹, a control algorithm based on Genetic Algorithms is compared to the standard P&O and IC. Unlike Yatimi et al.³⁰, that does this comparison with the control algorithms P&O and SMC, and Ramos-Hernanz et al.³¹ compares P&O, IC and SMC. A new control algorithm based on SMC was also presented in Ramos-Hernanz et al.³². In this study, the performance of the algorithm was simulated and compared with real tests. The results of the simulations showed good agreement with the experimental ones.

Another possible MPPT technique family are fuzzy logic based controllers^{33,34}. These studies use fuzzy logic based controllers with time delay voltages and currents. The relationship between different variables is done with fuzzy logic rules, being set or trained with real data.

Shahid et al.⁵ proposed an Incremental Conductance based algorithm for indoor PV system under controlled temperature conditions. An intermediate optical stage called temperature controller was introduced in the study to transport the temperature of the concentrated light and hereafter solar PV panel to Standard Test Conditions (STC). A MPPT based on variable step sized incremental conductance algorithm was inserted at load side to ensure the conditioned and better quality power at the output.

The highest of the power-voltage curve of the PV panel is usually expressed as MPP, which is identified by a search algorithm. Lately, multipurpose Maximum Power Point Tracking (MPPT) algorithms have been suggested and implemented for outdoor solar PV systems^{35–38}. Yadav et al.³⁹ and Zahedi⁴⁰ studied the effect of temperature on MPP of the solar panel and stated a reduction in maximum output power with increasing temperature. As the temperature of the PV material increases, the band gap of the semiconductor material is reduced giving more energy to the electrons. The lower band gap increases the carrier and therefore, the mobility of the carriers is reduced. They recombine before reaching the other electrode. The more the recombination the more saturation current. Thakur et al.⁴¹ investigated the need of open circuit voltage on temperature of the solar cell. Yadav et al.⁴² demonstrated that in low concentration PV systems, temperature is increased with high concentration of light and need an optic solution to balance the temperature effects. A detailed study about the effect of temperature on solar cell's open circuit voltage and the MPP for diverse temperatures was presented in Yadav et al.⁴².

In the current study, authors propose a new MPPT that uses only the PV temperature. An optimal current vs power curve can be defined for each temperature. This optimal curve is applied in order to achieve the MPP. In “[Problem statement](#)”, authors describe a PV system and its dynamics; the maximum power points are also calculated in this section. This analysis emphasizes the dependence between optimal current and temperature. In Section *Temperature based MPPT algorithm*, authors propose a control law that profits the dependence of maximum power and optimal current for a given temperature. In Section *Temperature based MPPT algorithm stability analysis*, the stability of the complete system is demonstrated by means of a proposed Lyapunov energy function. Finally, a section is dedicated to explain the conclusions of the present study.

Problem statement

Photovoltaic module model. The most import stage in temperature based MPPT stability analysis is the PV electrical behavior characteristics. In order to identify this electrical behavior, authors propose several measurements.

By varying the load connected to the PV modules, and keeping the temperature and irradiance constant, the current and voltage change, producing the characteristic curves of the PV modules, as shown in Fig. 1. Conceptually, the curve represents the combinations of current, power and voltage in which the PV module could operate.

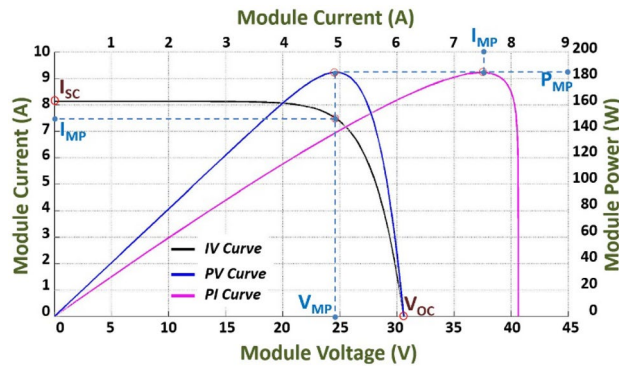


Figure 1. Mitsubishi Electric PV-TD185MF5 (185 Wp) PV module electrical characteristic.

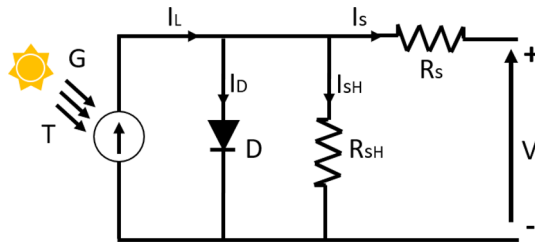


Figure 2. Equivalent circuit of a PV module.

The equivalent electrical circuit of a solar cell consists of a current source (I_L) dependent on irradiance. That irradiance is the current photo generated for a fixed value of solar radiation, a diode (D), a parallel resistance (R_{SH}) which is related to the imperfections of the union p-n and represents the leakage current and a series resistance (R_S). R_S represents the internal resistance of the material to the current flow and is associated with different effects such as the resistance of the contacts, of the semiconductors themselves and of the metallic diodes that form the frontal metallization mesh.

The mathematical model of the solar cell is obtained from its electrical representation and depends mainly on the solar radiation and the operating temperature of the cell.

By applying Kirchoff to the circuit illustrated in Fig. 2, the current generated by the PV module is determined by Eqs. (1) and (2):

$$I = I_L - I_D - I_{SH} \tag{1}$$

$$I = \underbrace{I_L}_{I_L} - I_0 \left(e^{\frac{q(V+IR_S)}{aKT_C}} - 1 \right) - \frac{I_{SH}}{R_{SH}} \tag{2}$$

where I is the output current of the solar cell, I_L is the photo generated current, I_D is the current through the diode, I_{SH} is the resistance loss current in parallel. I_0 is the inverse saturation current of the diode, q is the charge of the electron (1.6029×10^{-19} C), V is the voltage generated in the solar cell, K is the Boltzmann constant (1.3819×10^{-23} J/K), T_C is the operating temperature of the solar cell and a is the ideality factor.

The photo generated current varies depending on the solar radiation and the operating temperature of the solar cell, as described in Eq. (3):

$$I_L = \frac{G}{G_{Ref}} \left[I_{LRef} + \alpha_{ISC} (T_C - T_{CRef}) \right] \tag{3}$$

where G is the solar radiation at given conditions (W/m^2), G_{Ref} is the solar radiation at standard conditions ($1,000 W/m^2$), I_{LRef} is the current photo generating at reference conditions, which takes the value of the short-circuit current (I_{SC}). α_{ISC} is the short-circuit current temperature coefficient and T_{CRef} ($298^\circ K$) is the working temperature of the solar cell at standard conditions ($298^\circ K$).

The saturation current is responsible for some solar panel inefficiencies. Depending on the temperature it will increase as the solar cell temperature increases, lowering the efficiency, as is described in Eq. (4):

Parameter	Definition	Value [units]
N_s	Number of serial panels	50 [-]
N_p	Number of parallel panels	1 [-]
a	Ideality factor	1.805 [-]
q	Electron's charge	1.6×10^{-19} C
K	Boltzmann constant	1.38×10^{-23} J/°K
$T_{C_{ref}}$	Panel's reference temperature	298 °K
R_s	Series resistance	0.325 Ω
R_{sh}	Shunt resistance	218.37 Ω
G_{ref}	Solar radiation at reference conditions	1,000 W/m ²
$\alpha_{I_{SC}}$	Short-circuit current temperature coefficient	0.057%/°C
V_{OC}	Open circuit voltage	30.6 V
I_{SC}	Short circuit current	8.13 A
E_G	Band gap energy	30.6 J
I_{0Ref}	Inverse saturation current at reference conditions	3.84×10^{-10} A

Table 1. Model parameters.

$$I_0 = I_{0Ref} \left(\frac{T_C}{T_{C_{ref}}} \right)^3 e^{\left[\frac{qE_G}{aK} \left(\frac{1}{T_{C_{ref}}} - \frac{1}{T_C} \right) \right]} \quad (4)$$

where I_{0Ref} is the inverse saturation current at reference conditions and E_G is the band gap energy.

This inverse saturation current (I_{0Ref}) corresponds to the leakage of load carriers through the junction p-n, as a result of their recombination in a neutral zone of the semiconductor. It is calculated by Eq. (5):

$$I_{0Ref} = \frac{I_{SC}}{\left(e^{\frac{q(V_{OC})}{N_s a K T_C}} - 1 \right)} \quad (5)$$

Usually, the power produced by solar cells is low. Therefore, it is necessary to group them in series or parallel to achieve the desired power forming the PV module. Then, the coefficients N_p and N_s are added to Eq. (2) of a solar cell, which are the number of modules in parallel and the number of solar cells in series, respectively. The current-voltage characteristic equation of a solar panel is shown in Eq. (6):

$$I = N_s I_L - N_p I_0 \left(e^{\frac{q \left(\frac{V}{N_s} + \frac{I R_s}{N_p} \right)}{a K T_C}} - 1 \right) - \frac{V \left(\frac{N_p}{N_s} \right) + I R_s}{R_{SH}} \quad (6)$$

Equation (6) is reduced to Eq. (7), because shunt resistance does not affect the efficiency of a solar cell, since resistance tends to be very large or finite. Thus, $R_{SH} = \infty$ is assumed. However, the series resistance affects significantly the behaviour of the solar cell; therefore, for simple simulations the current provided by the solar panel described by Eq. (7):

$$I = N_s I_L - N_p I_0 \left(e^{\frac{q \left(\frac{V}{N_s} + \frac{I R_s}{N_p} \right)}{a K T_C}} - 1 \right) \quad (7)$$

Once the equations that model the behaviour of PV modules have been developed, the main parameters and variables of the Mitsubishi Electric PV-TD185MF5 (185 Wp) PV module are presented in Tables 1 and 2, respectively.

PV module characterization: maximum power vs temperature. The MPPT algorithm proposed in the current study consists on a parametrization of an optimal current function vs maximum power. This linear function depends on the temperature. Subsequently, the optimal current function for each temperature has been calculated.

The procedure is the following one. Firstly, the control measures the current, the generated power and temperature of the panel. The temperature has been used as variable, since the irradiance is much more expensive to measure than the temperature. In fact, the temperature is a smoother variable than the irradiance, thus the control does not need to change the optimal current function so quickly.

Thereafter, an optimal current function by the MPPT algorithm has been parametrized. That is, a function created from a linear regression performed with the optimal points (MPP) at each relation power-current.

By using this optimal current linear function, the algorithm calculates the current set point. In that way, the control forces the PV module to work in the optimal current line. Taking into account the dynamic of PV module,

Parameter	Definition	Units
I	Output current of the solar cell	A
V	Voltage generated in the solar cell	V
I_0	Inverse saturation current of the diode	A
T_C	Operating temperature of the solar cell	°C
I_L	Photo generated current	A
I_D	Current through the diode	A
I_{SH}	Resistance loss current in parallel	A

Table 2. Model variables.

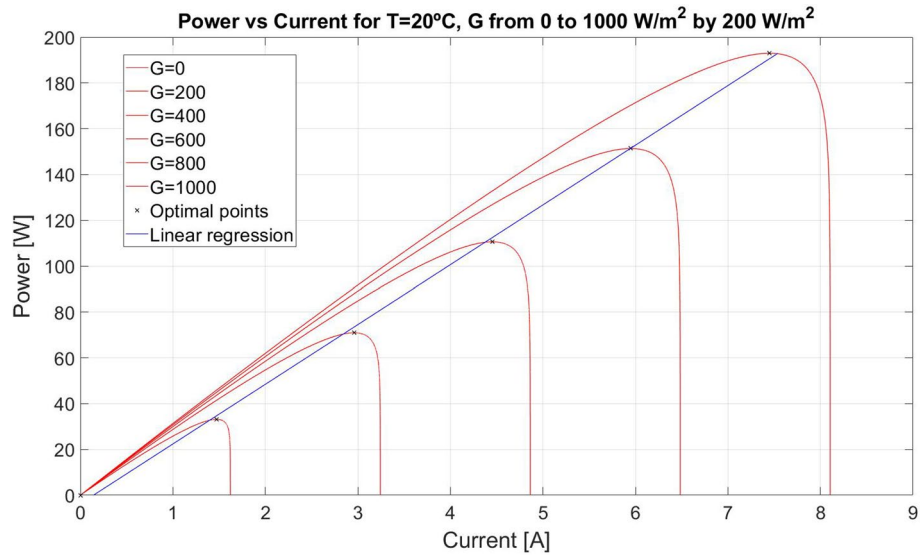


Figure 3. Maximum power vs optimal current for 20 °C.

the control always converges after several cycles to the optimal point. The stability of this MPPT algorithm has been verified in the next section in order to assure the convergence to this point.

Figure 3 shows different maximum power vs optimal current curves at 20 °C. Each curve is calculated for different irradiances with a constant temperature. The optimal points follow a line represented in blue colour in Fig. 3 and the coefficients of this line depend on temperature.

Thus, the blue line of Fig. 3 illustrates the MPP positions. Thereupon, if the control algorithm forces the PV module to work in this optimal line depending on temperature, the module dynamics converges to MPP.

The PV module output voltage depends on three variables: the module current (I), the irradiance (G) and the module temperature (T):

$$V = f(I, G, T) \tag{8}$$

This output voltage allows defining the output power (P) of the module:

$$P = V \cdot I = I \cdot f(I, G, T) \tag{9}$$

Besides, the PV module maximum power (P_{max}) values subject to a given temperature and irradiance can be calculated as shown in Fig. 4. The optimal current is a function of irradiance and temperature. If temperature is known, the maximum power and the optimal current depend on irradiance. Hence, power follows a curve that depends only on irradiance. Due to the optimal current dependence on irradiance, it can be defined a curve between maximum power and optimal current.

$$P_{max}(G, T) = \max_{s,t:G,T}(P(I, G, T)) \tag{10}$$

$$I_{optimal}(G, T) = \arg_{s,t:G,T}(P(I, G, T)) \tag{11}$$

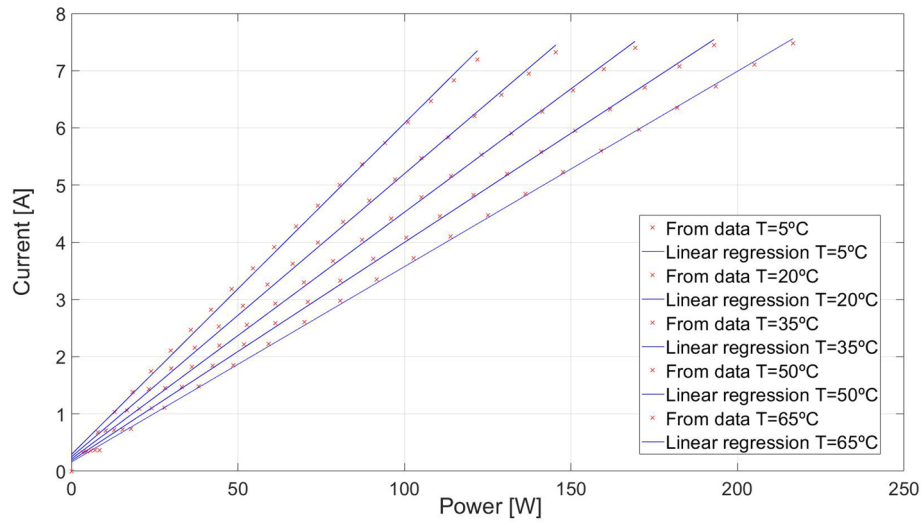


Figure 4. Maximum power vs optimal current curves for different temperatures.

Therefore, the real curve for a given temperature can be plotted. Finally, it can be stated that the optimal current for a given temperature for different irradiances follows a line. In order to make this affirmation the authors have proposed to eliminate the irradiance.

$$I_{optimal}(G, T) = F(P_{max}, T) \tag{12}$$

Hence, the MPPT algorithm presented in this paper must follow Eq. (12). If this equation is forced by the control, it can be said that the PV panel will operate in an optimal point.

Then a linear regression to specify the optimal current could be defined as in Eq. (13):

$$I_{optimal} = a(T) \cdot P_{max} + b(T) \tag{13}$$

Temperature based MPPT algorithm. The PV module dynamics is defined as a discrete time system, as the introduced MPPT algorithm works with t_k sample time. Thus, the MPPT algorithm generates a current set point. The panel achieves quickly the current set point, since the power electronics has a relay control with hysteresis. This relay control has a negligible dynamics; consequently, it is considered that the module output current at t_k instant is approximately the current set point, see Eq. (2):

$$P(t_k) = I(t_k) \cdot f(I(t_k), G(t_k), T(t_k)) \tag{14}$$

It is assumed that this control is able to measure the temperature and the obtained power. Therefore, following Eq. (13), the next sample time current $I(t_{k+1})$ is determined by Eq. (15):

$$I(t_{k+1}) = a(T(t_k)) \cdot P(t_k) + b(T(t_k)) \tag{15}$$

Equations (14) and (15) can be combined, resulting the equivalent system of Eq. (16):

$$I(t_{k+1}) = a(T(t_k)) \cdot [I(t_k) \cdot f(I(t_k), G(t_k), T(t_k))] + b(T(t_k)) \tag{16}$$

Consequently, the output current dynamics is summarized as follows in Eq. (17):

$$I(t_{k+1}) = F(I(t_k), G(t_k), T(t_k)) \tag{17}$$

Figure 5 shows the behaviour of this MPPT algorithm. The curve in red represents the dynamic function imposed by the MPPT, while the curve in blue illustrates the equilibrium line discussed in the following section.

Temperature based MPPT algorithm stability analysis. The whole system follows a discrete time equation (see Eq. (16)). Discrete time current equation has an equilibrium point that is defined by the intersection point between Eq. (16) and the line $I(t_{k+1}) = I(t_k)$. The discrete time current equation is in blue in Fig. 5.

The intersection point with line $I(t_{k+1}) = I(t_k)$ is a point that fulfils Eq. (15). Subsequently, there is only one point in Eq. (15) for each irradiance. Hence, if the discrete time current equation tends to a point of Eq. (15), this equilibria point is the MPP for that temperature and that irradiance.

Current equation is a first order discrete time system, therefore this equation has one equilibria point, see Fig. 5. On the one hand, it is well known that if the discrete time current equation is above line $I(t_{k+1}) = I(t_k)$ for I_k values less than the equilibria current I_e , then the output current will increase. In the other hand, if discrete

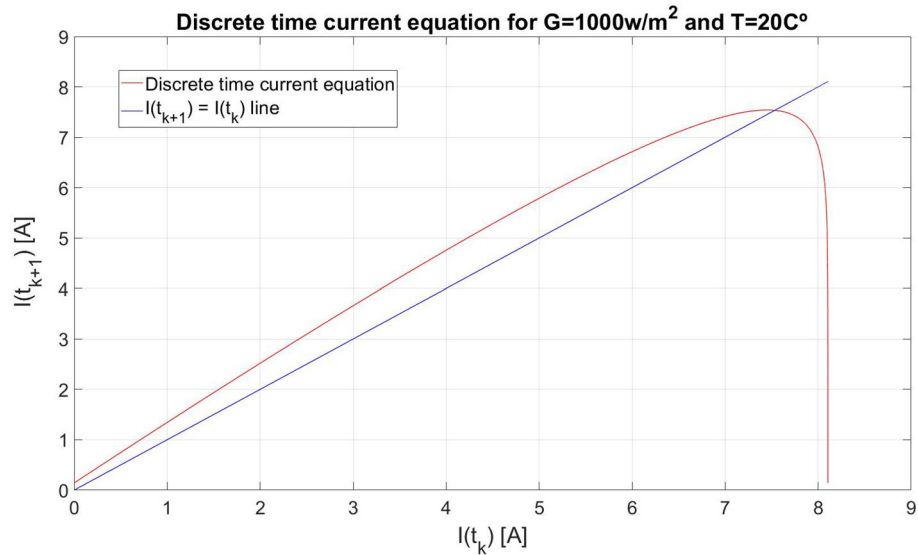


Figure 5. Discrete time current equation for 1000 W/m² irradiance and 20 °C temperature.

time equation is below line $I(t_{k+1}) = I(t_k)$, for I_k values bigger than the equilibria current I_e , then the output current will decrease, see Eqs. (18) and (19).

$$I(t_{k+1}) > I(t_k) \text{ if } I(t_k) < I_e \tag{18}$$

$$I(t_{k+1}) < I(t_k) \text{ if } I(t_k) > I_e \tag{19}$$

This behaviour has been experimentally evaluated for all temperature levels and irradiance. Only various cases are shown in order to introduce the general problem. Despite Eqs. (18) and (19), the stability of equilibria point is not completely proven because a first order discrete time system is not able to make damped oscillations around the equilibria point.

In order to prove the stability of this equilibria point, a Lyapunov based function is proposed. The Lyapunov function has to fulfil with several mathematical conditions in order to be a valid energy function. These conditions are:

1. $V(I(t_k)) > 0$ if $I(t_k) \neq I_e$
2. $V(I(t_k) = I_e) = 0$
3. $V(I(t_k))$ must be continue for all $I(t_k)$

If $V(I(t_k))$ is monotone negative respect to k , I_e will be stable.

$$\Delta V = V(I(t_{k+1})) - V(I(t_k)) < 0 \tag{20}$$

The function proposed in this work is the following one:

$$V(I(t_k)) = \begin{cases} (I(t_k) - I_e)^2, & \text{if } I(t_k) < I_e \\ 0, & \text{if } I(t_k) = I_e \\ K_v(I(t_k) - I_e)^2, & \text{if } I(t_k) > I_e \end{cases}$$

$$K_v = \frac{I_e^2}{(I_e - I_b)^2} \tag{21}$$

where constant K_v is defined in order to assure a negative difference in Lyapunov energy function. I_b is a $I(t_k)$ current level such that $I(t_{k+1})$ is equal to a value such that $I(t_{k+1}) + I(t_k) - 2I_e$ is equal to zero. This mathematical condition is necessary in order to assure that the proposed Lyapunov function is always positive, and its increment is always negative, see Eq. (20).

$$I(t_{k+1}) + I(t_k) - 2I_e = 0 \tag{22}$$

If Eqs. (22) and (17) are combined, the I_b current definition is obtained.

$$F(I_b, G, T) + I_b - 2I_e = 0 \tag{23}$$

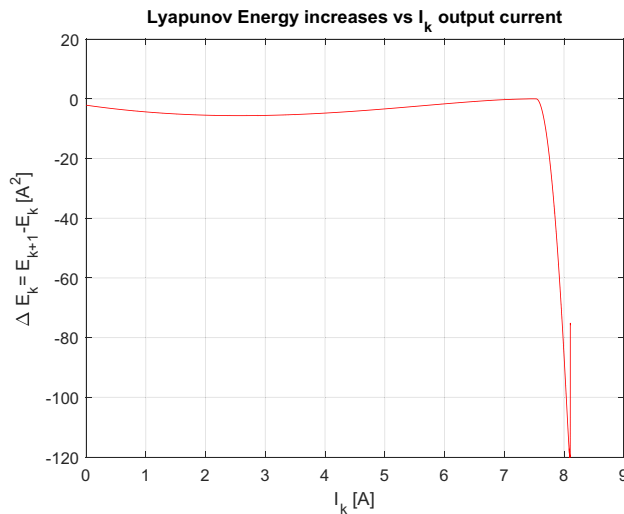


Figure 6. Lyapunov energy increments vs $I(t_k)$ for 1000 W/m² irradiance and 20 °C temperature.

The Lyapunov energy function increment is always negative for all $I(t_k)$ values. Different possible current spans are discussed in the following lines.

- 1) If $I(t_k) < I_e$, it is important to notice that the next current it is always less than I_e . because $I_e > I(t_{k+1})$. The following inequalities are fulfilled, which are verified in Fig. 5.

$$\Delta V = (I(t_{k+1}) - I_e)^2 - (I(t_k) - I_e)^2 = I(t_{k+1})^2 - I(t_k)^2 - 2I_e(I(t_{k+1}) - I(t_k))$$

Therefore, the Lyapunov functions increments are negatives for all t_k .

$$\Delta V = (I(t_{k+1}) - I(t_k))(I(t_{k+1}) + I(t_k) - 2I_e)$$

- 2) If $I(t_k) > I_e$, there are two different zones.
 - a) The first zone is defined by this condition: $I_e \leq I(t_{k+1})$. In this case, the Lyapunov energy function increment has an equivalent expression to Eq. (19).

$$\begin{aligned} \Delta V &= K_v(I(t_{k+1}) - I_e)^2 - K_v(I(t_k) - I_e)^2 \\ \Delta V &= K_v(I(t_{k+1}) - I(t_k))(I(t_{k+1}) + I(t_k) - 2I_e) \end{aligned} \tag{24}$$

In this zone the following inequality is fulfilled: $I(t_{k+1}) < I(t_k)$.

So $I_e \leq I(t_{k+1}) < I(t_k)$, and Lyapunov energy function increment is negative (see Eq. 24).

- b) In the second zone, when $I_e > I(t_{k+1})$ and $I(t_k) > I_e$, Lyapunov energy function increment has the following expression because $I(t_{k+1})$ is less than I_e .

$$\begin{aligned} \Delta V &= (I(t_{k+1}) - I_e)^2 - K_v(I(t_k) - I_e)^2 \\ \Delta V &= (I(t_{k+1}) - \sqrt{K_v}I(t_k))[(I(t_{k+1}) + \sqrt{K_v}I(t_k))] - 2I_e(I(t_{k+1}) - K_vI(t_k)) + (1 - K_v)I_e^2 \end{aligned} \tag{25}$$

Taking into account Eq. (21), ΔV from Eq. (25) takes always, negative values.

In Fig. 6, authors show Lyapunov energy function increment vs current $I(t_k)$. As it can be observed, all cases give negative values except to the equilibria point I_e .

Conclusions

The current work presents an innovative method to improve the efficiency of PV systems, consisting on PV modules temperature based MPPT algorithm.

P&O and Incremental Conductance based algorithms move the operating point to approach the MPP, although the working conditions are constant. The main advantage of these conventional algorithms is that they are adaptive and robust almost on any type of photovoltaic modules. However, the main disadvantage consists on their oscillating behavior around the MPP. Therefore, a loss of energy is obtained when the environmental conditions (irradiance and temperature) are constant, since they move the operating point around the MPP but they do not reach accurately the MPP.

One of the advantages of the Lyapunov based algorithm developed in the current study compared to other algorithms is that only one input is required for the control algorithm: the PV module temperature. On the contrary, other algorithms such as P&O and Incremental Conductance need to use more than one input. Therefore,

it makes our Lyapunov based algorithm easy to implement. Furthermore, this control law can be implemented into PV modules control system with a reasonably low cost.

The Lyapunov energy function based control algorithm presented in the current work forces the PV module to work along a linear function and in consequence, MPP is obtained in very few time steps. The number of cycles needed to achieve the optimal point are around 10, if the PV module starts in a very low current level (which is the worst case), as shown in Fig. 5. If the power electronics sample time is in the range between 10 to 1 ms, the time needed to achieve the optimal point is approximately from 100 to 10 ms. The stability of this MPPT algorithm has been determined in the present study via a Lyapunov energy function.

The most important drawback of this algorithm resides on the fact that an accurate PV model is required. Nevertheless, the PV module electronics needs to have an accurate model of PV in order to identify the dysfunctional states of PV modules.

As future work, the auto-tuning process of the photovoltaic panels should be developed. The PV modules used in the current work are well known by the authors; consequently, the MPPT algorithm presented in the current work is able to react very fast. However, in the case of using another type of PV modules, an algorithm to characterize immediately the necessary information required to adjust the MPPT is desirable. Moreover, additional research about how the MPPT based temperature control developed in the current work would behave in undesirable situations in photovoltaic panels such as partially shaded, failures or breakdowns is required. In addition, a PV module degradation study over time would be also interesting.

Received: 18 February 2020; Accepted: 23 June 2020

Published online: 27 July 2020

References

- Kulaksiz, A. A. & Akkaya, R. A genetic algorithm optimized ANN-based MPPT algorithm for a stand-alone PV system with induction motor drive. *Sol. Energy* **86**, 2366–2375 (2020).
- Manuel Lopez-Guede, J., Antonio Ramos-Hernanz, J., Zulueta, E., Fernandez-Gamiz, U. & Oterino, F. Systematic modeling of photovoltaic modules based on artificial neural networks. *Int J Hydrogen Energy* **41**, 12672–12687 (2016).
- Shahid, H. *et al.* Design and modeling of an optical band gap matched temperature controlled indoor concentrated light transmission system for photovoltaic energy production. *Optik* **176**, 502–511 (2020).
- Dang, H. & Singh, V. P. Nanowire CdS-CdTe solar cells with molybdenum oxide as contact. *Sci. Rep.* **5**, 14859 (2015).
- Shahid, H. *et al.* Implementation of the novel temperature controller and incremental conductance MPPT algorithm for indoor photovoltaic system. *Sol. Energy* **163**, 235–242 (2018).
- Putri, R. I., Wibowo, S. & Rifa'i, M. Maximum power point tracking for photovoltaic using incremental conductance method. in *2nd International Conference on Sustainable Energy Engineering and Application (Icseea) 2014 Sustainable Energy for Green Mobility* **68**, 22–30.
- Kumar, K. K., Bhaskar, R. & Koti, H. Implementation of MPPT algorithm for solar photovoltaic cell by comparing short-circuit method and incremental conductance method. in *7th International Conference Interdisciplinarity in Engineering (Inter-Eng 2013)* **12**, 705–715 (2014).
- Kamran, M. *et al.* Implementation of improved Perturb & Observe MPPT technique with confined search space for standalone photovoltaic system. *J. King Saud Univ. Eng. Sci.*
- Anto, E. K., Asumadu, J. A. & Okyere, P. Y. PID Control for Improving P&O-MPPT Performance of a Grid-Connected Solar PV System With Ziegler-Nichols Tuning Method. *Proceedings of the 2016 IEEE 11th Conference on Industrial Electronics and Applications (Icsea)*, 1847–1852 (2016).
- Sahnoun, M. A., Ugalde, H. M. R., Carmona, J. & Gomand, J. Maximum power point tracking using P&O control optimized by a neural network approach: a good compromise between accuracy and complexity. *Mediterranean Green Energy Forum 2013: Proceedings of an International Conference Mgef-13* **42**, 650–659.
- Faizal, A., Sutoyo, R., Mulyono, A. & Yendra, F. Design maximum power point tracking (MPPT) on photovoltaic panels using fuzzy logic method. *Am. J. Eng. Appl. Sci.* **9**, 789–797 (2016).
- Mao, M. *et al.* A two-stage particle swarm optimization algorithm for MPPT of partially shaded PV arrays. *Int. J. Green Energy* **14**, 694–702 (2017).
- Motahhir, S., El Hammoumi, A. & El Ghzizal, A. The most used MPPT algorithms: review and the suitable low-cost embedded board for each algorithm. *J. Clean. Prod.* **246**, 118983 (2020).
- Devi, V. K., Premkumar, K., Beevi, A. B. & Ramaiyer, S. A modified Perturb & Observe MPPT technique to tackle steady state and rapidly varying atmospheric conditions. *Sol. Energy* **157**, 419–426 (2017).
- Alik, R. & Jusoh, A. An enhanced P&O checking algorithm MPPT for high tracking efficiency of partially shaded PV module. *Sol. Energy* **163**, 570–580 (2018).
- Moshksar, E. & Ghanbari, T. A model-based algorithm for maximum power point tracking of PV systems using exact analytical solution of single-diode equivalent model. *Sol. Energy* **162**, 117–131 (2018).
- Ramos-Hernanz, J. A. *et al.* Study of the behavior of the Perturbation and Observation algorithm for MPPT (*International Conference on Technical and Physical Problems of Electrical Engineering*, 2016).
- Chen, Y., Lai, Z. & Liang, R. A novel auto-scaling variable step-size MPPT method for a PV system. *Sol. Energy* **102**, 247–256 (2014).
- Radjai, T., Rahmani, L., Mekhilef, S. & Gaubert, J. P. Implementation of a modified incremental conductance MPPT algorithm with direct control based on a fuzzy duty cycle change estimator using dSPACE. *Sol. Energy* **110**, 325–337 (2020).
- Ramos-Hernanz, J. A. *et al.* Study of the behavior of the Incremental Conductance algorithm for MPPT. *2016 8th International Conference on Electronics, Computers and Artificial Intelligence (Ecai)*.
- Rezk, H. & Eltamaly, A. M. A comprehensive comparison of different MPPT techniques for photovoltaic systems. *Sol. Energy* **112**, 1–11 (2020).
- Cortajarena, J. A., Barambones, O., Alkorta, P. & De Marcos, J. Sliding mode control of grid-tied single-phase inverter in a photovoltaic MPPT application. *Sol. Energy* **155**, 793–804 (2020).
- Chaieb, H. & Sakly, A. A novel MPPT method for photovoltaic application under partial shaded conditions. *Sol. Energy* **159**, 291–299 (2018).
- Li, S. A MPPT control strategy with variable weather parameter and no DC/DC converter for photovoltaic systems. *Sol. Energy* **108**, 117–125 (2020).
- Bayod-Rujula, A. & Cebollero-Abian, J. A novel MPPT method for PV systems with irradiance measurement. *Sol. Energy* **109**, 95–104 (2020).

26. Li, S., Liao, H., Yuan, H., Ai, Q. & Chen, K. A MPPT strategy with variable weather parameters through analyzing the effect of the DC/DC converter to the MPP of PV system. *Sol. Energy* **144**, 175–184 (2017).
27. El Khazane, J. & Tissir, E. H. Achievement of MPPT by finite time convergence sliding mode control for photovoltaic pumping system. *Sol. Energy* **166**, 13–20 (2018).
28. Mohapatra, A., Nayak, B., Das, P. & Mohanty, K. B. A review on MPPT techniques of PV system under partial shading condition. *Renew. Sustain. Energy Rev.* **80**, 854–867 (2020).
29. Hadji, S., Gaubert, J. & Krim, F. Theoretical and experimental analysis of genetic algorithms based MPPT for PV systems. in *International Conference on Technologies and Materials for Renewable Energy, Environment and Sustainability-Tmrees15* **74**, 772–787.
30. Yatimi, H. & Aroudam, E. MPPT algorithms based modeling and control for photovoltaic system under variable climatic conditions. in *11th International Conference Interdisciplinarity in Engineering, Inter-Eng 2017* **22**, 757–764.
31. Ramos-Hernanz, J., Manuel Lopez-Guede, J., Barambones, O., Zulueta, E. & Fernandez-Gamiz, U. Novel control algorithm for MPPT with boost converters in photovoltaic systems. *Int J Hydrogen Energy* **42**, 17831–17855 (2017).
32. Ramos-Hernanz, J. A. *et al.* Sliding mode real-time control of photovoltaic systems using neural estimators. *Int. J. Photoenergy*, 5214061.
33. Kwan, T. H. & Wu, X. Maximum power point tracking using a variable antecedent fuzzy logic controller. *Sol. Energy* **137**, 189–200 (2016).
34. Chen, Y., Jhang, Y. & Liang, R. A fuzzy-logic based auto-scaling variable step-size MPPT method for PV systems. *Sol. Energy* **126**, 53–63 (2020).
35. El Bahir, L. & Hassboun, T. Accurate Maximum power point tracking algorithm based on a photovoltaic device model. *Int. J. Photoenergy*, 5693941.
36. Farahat, M. A., Enany, M. A. & Nasr, A. Assessment of maximum power point tracking techniques for photovoltaic system applications. *J. Renew. Sustain. Energy* **7**, 042702 (2015).
37. Hong, Y. *et al.* Efficient maximum power point tracking for a distributed PV system under rapidly changing environmental conditions. *IEEE Trans. Power Electron.* **30**, 4209–4218 (2020).
38. Bhatnagar, A. P. & Nema, B. R. K. Conventional and global maximum power point tracking techniques in photovoltaic applications: a review. *J. Renew. Sustain. Energy* **5**, 032701 (2013).
39. Yadav, P., Tripathi, B., Lokhande, M. & Kumar, M. Estimation of steady state and dynamic parameters of low concentration photovoltaic system. *Solar Energy Mater. Solar Cells* **112**, 65–72 (2020).
40. Zahedi, A. Review of modelling details in relation to low-concentration solar concentrating photovoltaic. *Renew. Sustain. Energy Rev.* **15**, 1609–1614 (2011).
41. Thakur, A. K., Wantz, G., Garcia-Belmonte, G., Bisquert, J. & Hirsch, L. Temperature dependence of open-circuit voltage and recombination processes in polymer-fullerene based solar cells. *Solar Energy Mater. Solar Cells* **95**, 2131–2135 (2020).
42. Yadav, A. S., Pachauri, R. K. & Chauhan, Y. K. Comprehensive investigation of PV arrays with puzzle shade dispersion for improved performance. *Sol. Energy* **129**, 256–285 (2020).

Acknowledgements

“Development Agency of the Basque Country (SPRI) is gratefully acknowledged for economic support through the research project “Refrigeración de dispositivos de alto flujo térmico mediante impacto de chorro” (AIRJET), KK-2018/00109, Programa ELKARTEK.”

Author contributions

J.R.H. conceived the experiments, I.U. conducted the experiments, J.M.L.G., U.F.G. and A.M. analysed the results, and E.Z. conceived the theory. All authors reviewed the manuscript.

Competing interests

The authors declares no competing interests.

Additional information

Correspondence and requests for materials should be addressed to E.Z.

Reprints and permissions information is available at www.nature.com/reprints.

Publisher’s note Springer Nature remains neutral with regard to jurisdictional claims in published maps and institutional affiliations.



Open Access This article is licensed under a Creative Commons Attribution 4.0 International License, which permits use, sharing, adaptation, distribution and reproduction in any medium or format, as long as you give appropriate credit to the original author(s) and the source, provide a link to the Creative Commons license, and indicate if changes were made. The images or other third party material in this article are included in the article’s Creative Commons license, unless indicated otherwise in a credit line to the material. If material is not included in the article’s Creative Commons license and your intended use is not permitted by statutory regulation or exceeds the permitted use, you will need to obtain permission directly from the copyright holder. To view a copy of this license, visit <http://creativecommons.org/licenses/by/4.0/>.

© The Author(s) 2020